Strain and Near Attack Conformers in Enzymic Thiamin Catalysis: X-ray Crystallographic Snapshots of Bacterial Transketolase in Covalent Complex with Donor Ketoses Xylulose 5-phosphate and Fructose 6-phosphate, and in Noncovalent Complex with Acceptor Aldose Ribose 5-phosphate†

Peter Asztalos,▽ Christoph Parthier,▽ Ralph Golbik,‡ Martin Kleinschmidt,⊥ Gerhard Hübner,‡ Manfred S. Weiss,§ Rudolf Friedemann,|| Georg Wille,*,# and Kai Tittmann*,‡

Institut für Biochemie/Biotechnologie, Martin-Luther-University Halle-Wittenberg, Kurt-Mothes-Strasse 3, 06120 Halle/Saale, Germany, European Molecular Biology Laboratory Hamburg Outstation, c/o DESY, Notkestr. 85, 22603 Hamburg, Germany, and Institut für Organische Chemie, Martin-Luther-University Halle-Wittenberg

Received May 4, 2007; Revised Manuscript Received August 7, 2007

ABSTRACT: Transketolase is a prominent thiamin diphosphate-dependent enzyme in sugar metabolism that catalyzes the reversible transfer of a 2-carbon dihydroxyethyl fragment between a donor ketose and an acceptor aldose. The X-ray structures of transketolase from *E. coli* in a covalent complex with donor ketoses D-xylulose 5-phosphate (X5P) and D-fructose 6-phosphate (F6P) at 1.47 Å and 1.65 Å resolution reveal significant strain in the tetrahedral cofactor−sugar adducts with a 25−30° out-of-plane distortion of the C2−Cα bond connecting the substrates' carbonyl with the C2 of the cofactor's thiazolium part. Both intermediates adopt very similar extended conformations in the active site with a perpendicular orientation of the scissile C2−C3 sugar bond relative to the thiazolium ring. The sugar-derived hydroxyl groups of the intermediates form conserved hydrogen bonds with one Asp side chain, with a cluster of His residues and with the N4′ of the aminopyrimidine ring of the cofactor. The phosphate moiety is held in place by electrostatic and hydrogen-bonding interactions with Arg, His, and Ser side chains. With the exception of the thiazolium part of the cofactor, no structural changes are observable during intermediate formation indicating that the active site is poised for catalysis. DFT calculations on both X5P−thiamin and X5P-thiazolium models demonstrate that an out-of-plane distortion of the C2−Cα bond is energetically more favorable than a coplanar bond. The X-ray structure with the acceptor aldose D-ribose 5-phosphate (R5P) noncovalently bound in the active site suggests that the sugar is present in multiple forms: in a strained ring-closed β-D-furanose form in C2-*exo* conformation as well as in an extended acyclic aldehyde form, with the reactive C1 *aldo* function held close to Cα of the presumably planar carbanion/enamine intermediate. The latter form of R5P may be viewed as a near attack conformation. The R5P binding site overlaps with those of the leaving group moieties of the covalent donor-cofactor adducts, demonstrating that R5P directly competes with the donor-derived products glyceraldehyde 3-phosphate and erythrose 4-phosphate, which are substrates of the reverse reaction, for the same docking site at the active site and reaction with the DHEThDP enamine.

Thiamin diphosphate (ThDP[1], Figure 1A), the coenzyme derived from vitamin B_1, plays an important role in the mechanisms of many essential metabolic enzymes (*1*−*4*). As a prototype for the classic *Umpolung* mechanism, the electrophilic nature of the positively charged thiazolium nucleus of ThDP helps to stabilize carbanions of the cofactor (the ThDP ylide) and of derived substrate−cofactor intermediates. In that way, ThDP enzymes lower the activation

† This work was supported in part by Research Grant 0126FP/0705M from the Ministry of Education at Saxony-Anhalt (to K.T.) and the Degussa Foundation. We thank the Degussa Foundation and the Graduiertenförderung des Landes Sachsen-Anhalt for financial support to P.A.

* To whom correspondence should be addressed. Phone: ++49-345-5524887. Fax: ++49-345-5527014. E-mail: kai.tittmann@biochemtech.uni-halle.de (K.T.). E-mail: wille@biophysik.org (G.W.).

‡ Institut für Biochemie/Biotechnologie, Martin-Luther-University Halle-Wittenberg.

§ European Molecular Biology Laboratory Hamburg Outstation.

|| Institut für Organische Chemie, Martin-Luther-University Halle-Wittenberg.

⊥ Present address: Probiodrug AG, Halle, Germany.

Present address: Institut für Biophysik, Johann-Wolfgang-Goethe-Universität Frankfurt am Main, Max von Laue-Str. 1, 60438 Frankfurt, Germany.

▽ Both authors contributed equally to this work.

[1] Abbreviations: TK, transketolase; POX, pyruvate oxidase; PDH, pyruvate dehydrogenase; TIM, triosephosphate isomerase; G3PDH, *sn*-glycerol-3-phosphate/NAD^+ 2-oxido-reductase; X5P, xylulose 5-phosphate; F6P, fructose 6-phosphate; R5P, ribose 5-phosphate; E4P, erythrose 4-phosphate; G3P, glyceraldehyde 3-phosphate; S7P, sedoheptulose 7-phosphate; HPA, β-hydroxy-pyruvate; ThDP, thiamin diphosphate; X5P-ThDP, covalent adduct of X5P and ThDP; F6P-ThDP, covalent adduct of F6P and ThDP; S7P-ThDP, covalent adduct of S7P and ThDP; DHEThDP, 1,2-dihydroxyethyl-ThDP; LThDP, 2-lactyl-ThDP; DFT, density functional theory; B3LYP, Becke's three parameter exchange functional along with the Lee−Yang−Parr nonlocal correlation functionals.

10.1021/bi700844m CCC: $37.00
Published on Web 10/03/2007

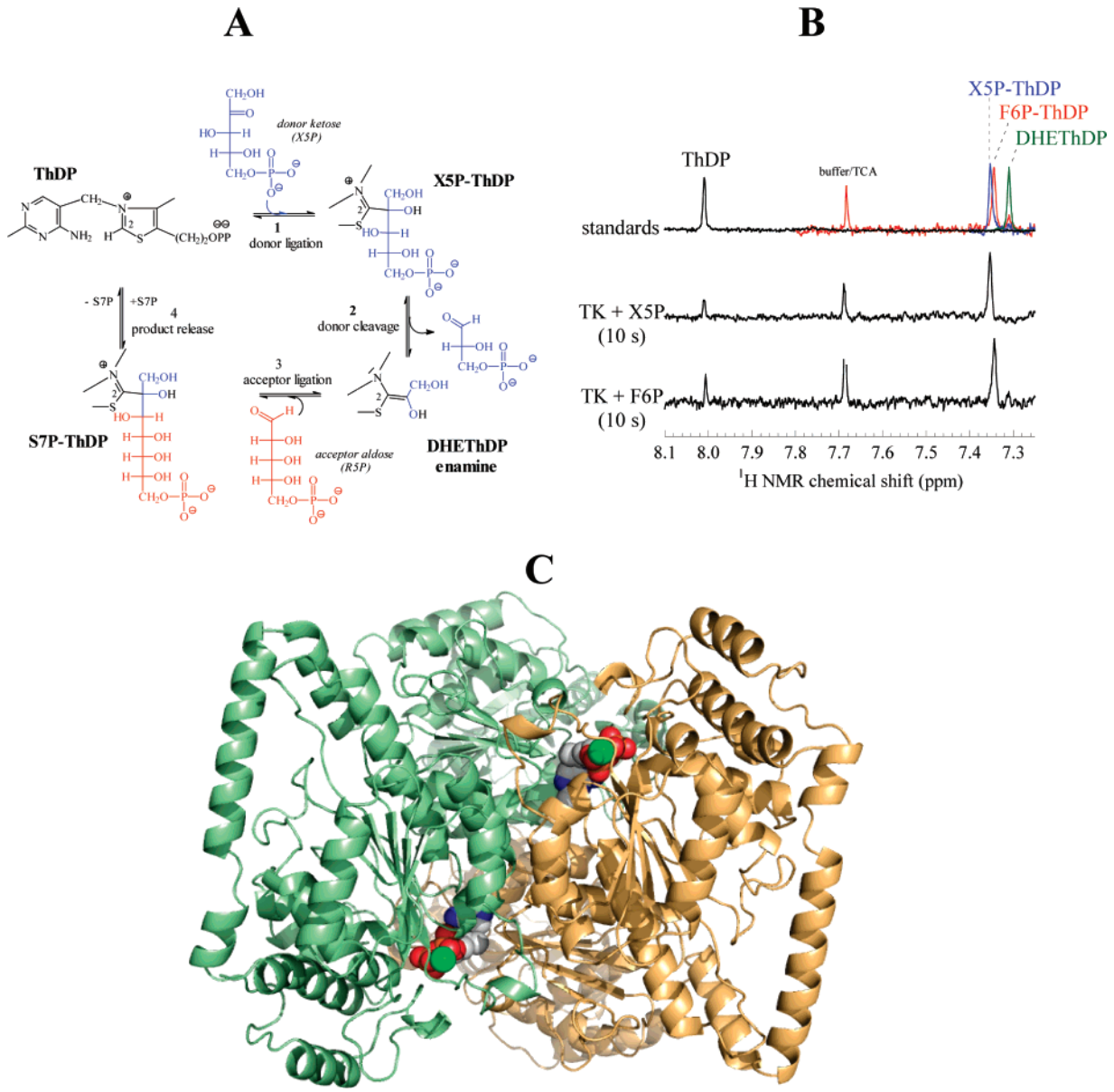

FIGURE 1: (A) Minimal reaction mechanism of transketolase for the conversion of donor ketose D-xylulose 5-phosphate (X5P) and acceptor aldose D-ribose 5-phosphate (R5P) yielding sedoheptulose 7-phosphate (S7P) and glyceraldehyde 3-phosphate (G3P) with intermediates and elementary steps of catalysis identified. A similar mechanism can be envisioned for the conversion of the alternative 6-carbon donor ketose D-fructose 6-phosphate (F6P) and D-ribose 5-phosphate, which results in the formation of the 4-carbon aldose erythrose 4-phosphate and sedoheptulose 7-phosphate. (B) ^{1}H NMR based analysis of the intermediate distribution after the reaction of TK with either xylulose 5-phosphate or fructose 6-phosphate for 10 s and subsequent acid quench isolation using the characteristic C6′-**H** proton signal of chemically and chemoenzymatically synthesized intermediates as standards (*20*). Identical intermediate distributions were observed for longer reaction times (60 s), suggesting a stabilization of the initial sugar−cofactor adduct on the enzyme (Supporting Information). (C) Structure of TK from *E. coli* (pdb code 1QGD). The cofactors ThDP and Ca^{2+} (green) are shown as spheres. The corresponding subunits of the dimer are colored individually.

barrier for reactions where carbon−carbon bonds are formed or cleaved, including, for instance, the decarboxylation of 2-ketoacids (pyruvate decarboxylase and pyruvate dehydrogenase) and carboligation of carbonyl substrates (acetohydroxyacid synthase and transketolase).

The ThDP-dependent enzyme transketolase (TK, EC 2.2.1.1) is found in all organisms and serves to connect the pentose phosphate pathway to glycolysis. In plants, TK is a key enzyme of the Calvin cycle of photosynthesis (*5*, *6*). TK catalyzes the reversible transfer of a 2-carbon fragment derived from ketose phosphates to the C1 position of aldose phosphates (Figure 1A). In the catalytic conversion of the physiological substrates D-xylulose 5-phosphate (X5P) and D-ribose 5-phosphate (R5P), the C2 carbanion of enzyme-bound ThDP first adds to the C2 keto function of X5P (*step 1*) yielding a covalent cofactor−substrate adduct. In the next step, the C2−C3 bond of the sugar phosphate is cleaved (*step 2*) to give the 1,2-dihydroxyethyl-ThDP (DHEThDP) intermediate, presumably stabilized in its planar enamine form (*7*), and glyceraldehyde 3-phosphate (G3P). After the binding of the acceptor R5P to the active site, the reactive enamine will covalently add to the C1 *aldo* function of R5P (*step 3*), followed by the elimination (*step 4*) of the resultant 7-carbon ketose sedoheptulose 7-phosphate (S7P).

The structure and mechanism of TK have been studied in detail by the pioneering work of Schneider, Lindqvist, and

co-workers (*5*). TK is a homodimeric protein with two active sites. The cofactors ThDP and Ca^{2+} are bound at the subunit interface (Figure 1C). Notably, after reaction of the enzyme with the artificial substrate β-hydroxy-pyruvate (HPA), the three-dimensional structure of the DHEThDP intermediate trapped in the active site could be characterized and suggested a planar enamine-like form with *E*-configuration (*7*). Cocrystallization of TK with the donor ketose fructose 6-phosphate (F6P) allowed the observation of the 4-carbon acceptor aldose erythrose 4-phosphate bound in a docking site of TK as a result of enzyme-catalyzed decomposition of F6P (*8*). In-depth mutagenesis studies helped to delineate the catalytic and binding functions of individual active site residues (*9*−*12*). Despite these major achievements, the structures of some catalytic key intermediates have remained elusive.

Most importantly, an initial covalent complex of enzyme-bound ThDP with a donor ketose could not be structurally characterized so far. Recent studies on related ThDP enzymes that act on the 2-keto acid pyruvate provided evidence for a stereoelectronically controlled elimination of the product CO_2 and some strain in the tetrahedral substrate−cofactor adducts, varying from 7 to 11° of distortion of the bond formed between the sp^2 C2 of ThDP and the sp^3 carbon 2 of the substrate relative to the planar aromatic thiazolium ring (*13*, *14*). It has been suggested that this strain exerted on the intermediate is an important driving force of the reaction because it will be eventually relieved in the course of product elimination, yielding the planar, unstrained carbanion/enamine intermediate. Also, the carboxylate leaving group was shown to bind in a hydrophobic microenvironment, which is considered to facilitate the elimination of the product CO_2 (*13*). In TK, the polarity of the active site may not be as important as that for enzymes that release CO_2 because all TK substrates and products are sugar phosphates and exhibit very similar chemical properties. Therefore, other driving forces must account for C2−C3 bond cleavage of the donor ketose.

A second important issue is the adaptation of the enzyme's active site to bind sugar phosphates of different length. Aside from the 5-carbon donor ketose X5P and the 7-carbon ketose S7P (the substrate of the reverse reaction), TK may alternatively use the 6-carbon ketose D-fructose 6-phosphate (F6P) as a substrate, yielding erythrose 4-phosphate and the DHEThDP enamine. It is still unknown what interactions of the sugar phosphates in the active site determine substrate specificity and whether there are different binding patterns for the phosphate moiety of the substrates with 5-carbon, 6-carbon, or 7-carbon chain length.

Finally, TK encounters a problem specifically related to the intrinsic chemical nature of its sugar substrates. With the exception of X5P, all other substrates of TK are thermodynamically stabilized in the cyclic semiacetal form in free solution. The equilibrium fraction of the reactive acyclic C1 *aldo* form (R5P) or 2-keto form (F6P) accounts for only 2.5% (F6P) or even less as in the case of ribose with an estimated carbonyl fraction of 0.05−0.10% (*15*−*18*). Therefore, TK must find ways to stabilize the acyclic forms of its substrates to ensure catalysis.

Here, we report the high-resolution X-ray structures of the hitherto elusive initial covalent X5P and F6P sugar−cofactor adducts, and of the noncovalent complex with the acceptor R5P, all trapped in the active site of TK from *E. coli*. These crystallographic snapshots allow the formulation of a molecular chemical mechanism and shed new light on the mode of action of TK.

MATERIALS AND METHODS

Bacterial Strain and Plasmid. The plasmid pGSJ427 encoding for transketolase A (TKA) from *Escherichia coli* was kindly provided by Professor Georg Sprenger (University of Stuttgart, Germany). The insertion of an C-terminal His_6-tag to *tktA* and gene sequencing were carried out using standard molecular biology techniques and will be described in full detail elsewhere (Asztalos et al., manuscript in preparation). *E. coli* strain JM109 (New England Biolabs) was used for the expression of *tktA* wild type. The protein double variant His26Ala/His261Ala was generated by two-step site-directed mutagenesis using the QuikChange-Kit (Stratagene, USA). Plasmid pGSJ427 containing the wild-type gene of bacterial transketolase A (*tktA*) with a C-terminal His_6-tag was used as template DNA. Mutagenesis of His26 to Ala was carried out using the primer pair 1 + 2, the corresponding exchange of His261 using primer pair 3 + 4. The correctness of the mutation was confirmed by complete sequencing of the gene and mass spectrometric analysis of the purified enzyme variant.

Primer 1 (forward): GCC AAA TCC GGT GCG CCG GGT GCC CCT ATG.

Primer 2 (reverse): CAT AGG GGC ACC CGG CGC ACC GGA TTT GGC.

Primer 3 (forward): CAC GAC TCC GCG GGT GCG CC.

Primer 4 (reverse): GG CGC ACC CGC GGA GTC GTG.

Gene Expression and Protein Purification. The constructed plasmid pGSJ427 carrying the gene for TKA/His6-tag was transformed in *E. coli* JM 109 by electrotransformation. Cells were grown overnight at 37 °C in LB medium supplemented with 100 μg/mL ampicillin. In brief, protein purification was performed according to a modified protocol of that given in ref *19* and included (i) cell disruption using a French Press apparatus, (ii) removal of nucleic acids by streptomycin sulfate precipitation, (iii) Ni-NTA agarose affinity chromatography (Qiagen), and (iv) gel filtration (Superdex 75, Amersham). The purity of the protein was estimated to be >95% as determined by SDS−PAGE. The correct molecular weight of the protein was confirmed by MALDI/TOF mass spectrometry. A comparison of TKA and TKA-His_6 revealed no differences of the apparent dissociation constant of ThDP and of the steady-state kinetic constants. A detailed description of expression, purification, and biochemical properties of TKA-His_6 will be described elsewhere (Asztalos et al., manuscript in preparation).

Analysis of Covalent Substrate-ThDP Intermediates by Chemical Quench/^{1}H NMR Spectroscopy. The reactions of TK with the donor ketoses X5P and F6P in the absence and presence of the acceptor R5P were analyzed by a combined acid quench/^{1}H NMR method as detailed in ref *20*. The relative concentrations of the intermediates were estimated by ^{1}H NMR spectrocopy using the C6′-**H** proton signals of ThDP (8.01 ppm), of chemically synthesized DHEThDP

(7.31 ppm), and of chemoenzymatically synthesized X5P-ThDP (7.35 ppm) and F6P-ThDP (7.34 ppm) adducts as standards (see Figure 1B).

In a typical experiment, 15 mg/mL *apo*-enzyme (205 μM active sites) were reconstituted with an equimolar amount of ThDP and 5 mM $CaCl_2$ in 50 mM glycyl-glycine at pH 7.6. Under these conditions and taking into account a cofactor's dissociation constant of 0.1 μM (determined by fluorescence titration experiments), approximately 98% of the active sites are occupied with ThDP in dynamic equilibrium. Reconstituted *holo*-TK was then mixed with substrate solution (50 mM X5P or 50 mM F6P in 50 mM glycyl-glycine at pH 7.6) in a 1 + 1 mixing ratio for defined reaction times (1−60 s) at 8 °C. These experiments showed the equilibrium of reversible donor binding and cleavage (steps 1 and 2 in Figure 1A) to be established after a reaction time of 10 s.

In order to analyze the intermediate distribution during turnover of both the donor and the acceptor, TK was reacted with saturating concentrations of X5P/F6P plus R5P. For that purpose, 30 mg/mL *holo*-TK (410 μM active sites supplemented with 410 μM ThDP and 10 mM $CaCl_2$ in 50 mM glycyl-glycine at pH 7.6) was first premixed with donor substrate (100 mM X5P or 100 mM F6P) in a 1 + 1 mixing ratio at 8 °C. After 10 s of reaction time, which ensured quasi-equilibrium conditions for the donor half-reaction, 50 mM R5P (in 50 mM glycyl-glycine at pH 7.6) was added and allowed to react for a further 10 s. The reaction was then stopped by the addition of TCA/HCl as detailed in ref *20*. NMR data acquisition and processing were performed as described previously (*20*).

Kinetic Examination of EcTK Catalysis by a Coupled Enzymatic Assay. In addition to the kinetic NMR studies on the reaction of TK with X5P and F6P in the absence and presence of R5P, we studied the enzyme-catalyzed conversion of X5P with acceptor R5P in a spectrophotometric steady-state assay using the auxiliary enzymes triosephosphate isomerase (TIM) and *sn*-glycerol-3-phosphate/NAD^+ 2-oxido-reductase (G3PDH) to detect the formation of G3P, which is derived from the cleavage of X5P (*19*). The concomitant oxidation of NADH was followed spectrophotometrically at 25 °C and 340 nm in 50 mM glycyl-glycine at pH 7.6 supplemented with 0.3 mM ThDP and 2.5 mM Ca^{2+}. Activity of TK was determined at different fixed R5P and X5P concentrations and analyzed in double-reciprocal plots (1/v vs 1/substrate).

Isothermal Titration Calorimetry Experiments. Binding of the acceptor R5P to TK in the absence of donor was analyzed by isothermal titration calorimetry (ITC) using a high precision VP-ITC titration calorimetric system (Microcal Inc. Northampton, MA). For that purpose, TK (reconstituted with 1 mM ThDP and 5 mM Ca^{2+} in 50 mM glycyl-glycine buffer at pH 7.9) was first exhaustively dialyzed against buffer at 4 °C. R5P was diluted in the same buffer at a final concentration of 10 mM. *Holo*-TK (100 μM active sites in the same buffer as indicated above) was then placed in the sample cell and titrated with R5P (10 μL per injection, stock concentration 10 mM) at 8 °C, the same temperature that was also used for the substrate-soaking experiments/X-ray structural analysis of the R5P−TK complex (see next section). In order to correct for heat effects not directly related to the binding reaction of R5P to TK, control experiments were performed by injections of R5P into the sample cell containing only buffer.

DFT Calculations. Density functional theory (DFT) calculations on the B3LYP-6-31G(d) level were performed on simplified models of the X5P-ThDP complex using the program package GAUSSIAN98 (*21*). The aim of these calculations was to correlate energetic and structural features of the strained tetrahedral sugar−cofactor adduct observed in the X-ray crystal structures. Within the calculations, the X5P−thiamin (X5P-Th) and X5P−thiazolium (X5P-Thiaz) complex conformers were considered with a C2−Cα bond being either out-of-plane, as experimentally determined in the X-ray structural studies, or in-plane (torsional angle C5−S1−C2−Cα = 180°). Starting from the X-ray structure of X5P-ThDP trapped in the active site of TK, single point and full optimization calculations were carried out both for the model X5P-Th and X5P-Thiaz complexes. In addition, calculations with a partial optimization were carried out where the experimentally observed out-of-plane distortion of the C2−C2α bond and the torsion angles of the sugar's main chain were retained by appropriate constraints. The single protonated form for the phosphate group of the sugar was used so that all model complexes are formally charge-neutral. In case of X5P-Th, the aminopyrimidine moiety was modeled as the 1′,4′-imino tautomer, which is supposed to be stabilized on ThDP enzymes in tetrahedral substrate−cofactor adducts (*22*).

X-ray Crystallography. Crystals of TK-His_6 (in 50 mM glycyl-glycine, 10 mM ThDP, and 5 mM $CaCl_2$ at pH 7.9) were grown in hanging drops in a volume of 6 μL using the vapor diffusion method against a reservoir solution containing 19−22% (w/v) PEG 6000 and 1% (v/v) glycerol as precipitants (*7*, *23*).

Typically, crystal growth occurred at 8 °C within 4−6 weeks. Before flash-cooling a crystal in liquid nitrogen, it was incubated in a cryosolution with 20% (w/v) PEG 6000 and 20% (v/v) ethylene glycol in 50 mM glycyl-glycine, 10 mM ThDP, and 5 mM $CaCl_2$ at pH 7.9 and was additionally supplemented with substrate, either X5P or F6P or R5P. For the experiments with the donor ketoses, crystals were soaked with 25 mM X5P or 25 mM F6P for 15−25 s at 8 °C, conditions under which the overall equilibrium of donor binding and cleavage (steps 1 and 2 in Figure 1A) is established according to NMR intermediate analysis. For the structural characterization of TK in complex with the physiological acceptor R5P, crystals were soaked with 25 mM R5P at 8 °C for 1 min.

X-ray datasets of TK in covalent complex with X5P and F6P were collected from a single crystal at cryogenic temperatures at beamline BW7B, European Biological Molecular Laboratory outstation, Deutsches Elektronen Synchrotron Hamburg. The dataset of TK in noncovalent complex with acceptor R5P was collected from a single crystal in a 100 K cryostream using our in-house facilities (Rigaku, Japan) in the Institute of Biochemistry & Biotechnology of Halle University. The diffraction data extended to a resolution of 1.47 (covalent cofactor complex with X5P), 1.65 (covalent cofactor complex with F6P), and 1.60 Å (noncovalent complex with R5P), respectively.

Crystallographic datasets were processed with Denzo/Scalepack (*24*) or Mosflm (*25*). Initial phases were obtained through molecular replacement with the program Molrep or

Amore (*26*) and by using the wild-type structure of TK from *E.coli* (pdb code 1qgd) as a search model. Inspection of electron density maps, model building, and multiple refinement cycles were conducted with Refmac5 (*26*) and Coot (*27*) until the free *R*-factor and the crystallographic *R*-factor had converged.

Modeling of the protein-bound ligands X5P-ThDP and F6P-ThDP (the covalent adducts of the donor sugars and ThDP) was carried out as follows: even though electron density omit maps had already indicated a covalent sugar−ThDP adduct in the active site of TK, initial refinement trials were performed with separate entities of the donor sugar substrate (X5P or F6P) and ThDP, that is, with the sugar substrate prior to the cofactor's nucleophilic attack. As the difference density maps showed that the C2 carbon of the sugar was unlikely to be planar, that is, not sp^2-hybridized, and the distance between C2 of the sugar and C2 of the thiazolium ring was too small for a van-der-Waals contact, covalent ligand moieties were introduced for refinement. The geometry of the ThDP−sugar adduct was derived as follows: the molecule was constructed by the addition of the sugar phosphate part to the monomer library entry of ThDP in the CCP4 program package. Subsequent regularization with REFMAC5 yielded a covalent adduct that had the tetrahedral, that is, sp^3-hybridized C2 carbon atom of the sugar in the plane of the aromatic thiazolium ring, at a C2(sugar)−C2(thiazolium) bond length of 1.50 Å (the same as that for the 4-methyl group attached to the thiazolium ring). This ligand was introduced into the protein structure using COOT. Subsequent refinement trials systematically revealed difference density clearly favoring a position of the sugar C2 carbon out-of-plane from the thiazolium ring. The REFMAC5 ligand description was therefore modified by removing the in-plane restraint for the C2 carbon of the sugar and by relaxing the accompanying angle restraints for the C2(sugar)−C2(thiazolium)−S(thiazolium) and C2(sugar)−C2(thiazolium)−N(thiazolium) angles, which would otherwise have forced the C2 of sugar to remain in ring plane. Also, no torsion restraints were imposed on the C2(sugar)−C2(thiazolium) bond and all bonds (length, angles, and torsion angles) between the thiazolium atoms of the covalent intermediates. Further refinement cycles yielded the geometry described here, which corresponds very well with the observed electron density. In the case of the F6P-ThDP adduct, the occupancy of the sugar atoms was estimated to be only 0.8 on the basis of the difference electron density, and this value was used in the final refinement cycles. In addition, unreacted ThDP with an occupancy of 0.2 was included in the model.

Structure refinement of the noncovalent complex with acceptor R5P was carried out using standard monomer libraries for ThDP, and the cyclic and acyclic forms of R5P. Crystallographic statistics are given in Table 1. Crystallographic figures were prepared with Pymol (*28*).

DATABASE ACCESSION NUMBER

The refined model and the corresponding structure factor amplitudes have been deposited in the Research Collaboratory for Structural Biology (http://www.rcsb.org) under accession numbers 2R8O (TK + X5P), 2R8P (TK + F6P), and 2R5N (TK + R5P).

RESULTS AND DISCUSSION

^{1}H NMR-Based Intermediate Analysis of the Reaction of TK with Physiological Donor Ketoses X5P/F6P and with the Artificial Donor HPA. When only the donor substrate is present, TK catalysis is restricted to the donor half-reaction (steps 1 and 2 in Figure 1A). At first, the donor substrate will form an initial covalent adduct with the enzyme-bound cofactor (step 1), followed by the elimination (step 2) of either a 3-carbon (G3P, reaction with X5P) or 4-carbon (E4P, reaction with F6P) aldose to yield the DHEThDP carbanion/enamine intermediate. In theory, in the absence of acceptor, an equilibrium over steps 1 and 2 should be established with stable fractions of (a) ThDP, (b) X5P-ThDP or F6P-ThDP, and (c) DHEThDP. Once the DHEThDP enamine intermediate is formed, it will be kinetically stabilized on the enzyme, that is, the off-pathway protonation of Cα and subsequent release of glycolaldehyde are slow (*29*).

Now, our intermediate studies on bacterial TK in the presence of 25 mM X5P show (Figure 1B) that under equilibrium conditions approximately 90% of all active sites are occupied by the covalent sugar−cofactor adduct X5P-ThDP. The remaining 10% active sites contain unreacted cofactor. Surprisingly, we could not observe the DHEThDP intermediate, implying its equilibrium concentration to be less than 5%. This observation suggests that the initial sugar−ThDP adduct in TK either does not decompose at all (or very slowly) in the absence of acceptor, that is, is stabilized on the enzyme, or the reverse reaction, the ligation of G3P to the DHEThDP enamine, is significantly faster than the forward reaction under the chosen conditions. However, one has to keep in mind that at most ≈100 μM G3P can be released from the X5P-ThDP intermediate (the active site concentration after 1 + 1 mixing of 205 μM enzyme with substrate). In view of the estimated apparent K_M for G3P under steady-state conditions of 2.1 mM (*19*), it is questionable if the enzyme could be indeed saturated at this low acceptor concentration of 0.1 mM when considering fast equilibrium conditions.

A similar scenario emerges for the reaction of TK with the alternative donor ketose F6P. In the presence of 25 mM of the sugar, approximately 75% of all active sites contain the covalent F6P-ThDP adduct, and 20% of active sites are occupied by unreacted ThDP. Contrary to the reaction of TK with X5P, very small amounts (≤5%) of the DHEThDP enamine intermediate could be detected. This is intriguing because decomposition of F6P-ThDP in TK will yield DHEThDP and E4P, which has been shown to be the best acceptor for *Ec*TK exhibiting an apparent K_M of 90 μM (*19*). If indeed the initial sugar−ThDP adduct would partition in two rapid equilibria (steps 1 and 2), one should, in theory, expect a higher F6P-ThDP concentration relative to DHEThDP than for the similar reaction with X5P because E4P (K_M^{app} = 90 μM) is by far the better acceptor than G3P (K_M^{app} = 2.1 mM). In order to dissect whether the initial covalent sugar−ThDP adducts X5P-ThDP and F6P-ThDP are kinetically stabilized on the enzyme in the absence of acceptor (slow cleavage of the adducts) or, alternatively, whether they are thermodynamically stable in rapid equilibria established over steps 1 and 2 (Figure 1A), we have conducted additional NMR experiments. At first, an analysis of the intermediate distribution after 60 s of reaction time (Supporting Informa-

Table 1: X-ray Crystallographic Statistics of Structures of TK from *E. coli* in Complex with Different Substrates

	TK + X5P	TK + F6P	TK + R5P
	data collection		
wavelength (Å)	0.8423	0.8423	1.5418
beamline	BW7B (EMBL Hamburg)	BW7B (EMBL Hamburg)	home source (rotating anode)
space group	$P2_12_12_1$	$P2_12_12_1$	$P2_12_12_1$
cell dimensions			
a (Å)	90.14	90.21	89.97
b (Å)	101.95	101.86	101.74
c (Å)	133.26	133.35	132.86
resolution (Å) (high res. shell) (Å)	27.40−1.47 (1.49−1.47)	40.47−1.65 (1.67−1.65)	35.00−1.60 (1.69−1.60)
R_{merge}	0.067 (0.318)	0.083 (0.535)	0.109 (0.66)
I/σ (I)	36.8 (8.1)	29.8 (6.1)	18.7 (3.8)
completeness (%)	99.8 (99.2)	99.5 (98.0)	99.3 (97.5)
redundancy	11.3	7.2	12.7
B-factor from Wilson plot (Å^2)	9.7	10.9	16.7
	refinement		
resolution (Å) (high res. shell) (Å)	27.14−1.47 (1.51−1.47)	39.87−1.65 (1.69−1.65)	35.00−1.60 (1.64−1.60)
no. reflections (work/test set)	205,715/2094	144,821/2182	151,746/8028
R_{work}	0.150	0.156	0.163
R_{free}	0.164	0.180	0.196
no. of atoms	11582	11282	12029
protein	10254	10207	10241
ligands	126	122	160
water	1202	953	1628
average *B*-factors (Å^2)			
protein	7.9	7.7	10.5
ThDP	8.4	8.4	13.0
sugar	X5P: 11.9	F6P: 15.7	R5P: 11.7
1,2-ethanediol	18.3	17.5	22.0
water	18.3	14.7	23.4
r.m.s deviations			
bond lengths (Å)	0.008	0.010	0.01
bond angles (°)	1.280	1.347	1.23
Ramachandran plot (%)			
favored	90.0	90.0	90.0
allowed	10.0	10.0	10.0

tion, Figure S1) reveals an intermediate pattern similar to that observed after 10 s (Figure 1B). As no DHEThDP (≤5%) intermediate can be detected, it may be concluded that either X5P-ThDP is very long-lived with $t_{1/2} > 10$ min or that the donor half-reaction is in equilibrium at 10 *and* 60 s. In another experiment, we reacted *Ec*TK with saturating amounts of X5P in the presence of 0.25 mM NADH and the enzymes triosephosphate isomerase (4.5 U) and *sn*-glycerol-3-phosphate/NAD^+ 2-oxido-reductase (1.55 U). If X5P-ThDP would be in a rapid equilibrium with DHEThDP and the product G3P, at least some fraction of the latter should be pulled out of equilibrium by TIM and G3PDH, eventually shifting the equilibrium toward the DHEThDP enamine intermediate by G3P removal. No DHEThDP intermediate should be detectable in case of a kinetic stabilization of X5P-ThDP on the enzyme. Now, the intermediate analysis after the reaction of *Ec*TK with 25 mM X5P for 10 s in the presence of TIM, G3PDH, and NADH (Supporting Information, Figure S2) clearly indicates the formation of DHEThDP, suggesting that X5P-ThDP is in rapid equilibrium with DHEThDP and G3P.

In an independent approach, we have studied the kinetic mechanism of the TK-catalyzed conversion of X5P and R5P in a spectrophotometric steady-state assay. Whereas a long-lived donor−ThDP adduct in the absence of acceptor would suggest a sequential mechanism, a Ping−Pong mechanism can be expected in the case of rapid equilibrium conditions for the donor-only reaction (steps 1 and 2 in Figure 1A). The double-reciprocal plot $1/v$ versus $1/S$ (Supporting Information, Figure S3) is clearly indicative for a Ping−Pong mechanism, although at very high concentrations of either substrate, a slight deviation from parallelism of the regression lines can be observed, presumably caused by direct competition of donor and acceptor, as also observed for TK from rat liver (*30*).

Contrary to the apparent stabilization of the covalent sugar−ThDP adducts X5P-ThDP and F6P-ThDP on the enzyme, the artificial substrate β-hydroxy-pyruvate (HPA) is rapidly converted by *Ec*TK to CO_2 and DHEThDP enamine in the absence of acceptor as also described for the yeast enzyme (*7*). The kinetic analysis of the reaction of *Ec*TK with HPA under single-turnover conditions by stopped-flow kinetics and quenched-flow/^{1}H NMR spectroscopy (Supporting Information, Figure S4) reveals that the DHEThDP enamine is rapidly formed with $t_{1/2} \approx 250$ ms and will be then very slowly converted to glycolaldehyde and ThDP ($t_{1/2} \approx 200$ s) in a nonproductive side reaction. The transiently formed tetrahedral HPA-ThDP adduct cannot be detected at any time point of the reaction, implying that it is very short-lived and not stabilized on the enzyme. This obvious

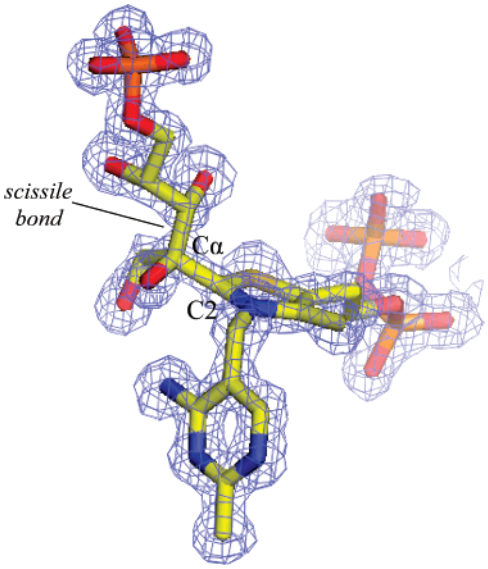

FIGURE 2: X-ray structure of the initial X5P-ThDP intermediate trapped in the active site of TK from *E. coli* after covalent addition of donor ketose xylulose 5-phosphate to C2 of enzyme-bound ThDP. The electron density is contoured at 1.3σ in a $2F_o - F_c$ map. The structure suggests an 25−30° distortion of the C2−Cα bond out of the thiazolium ring plane.

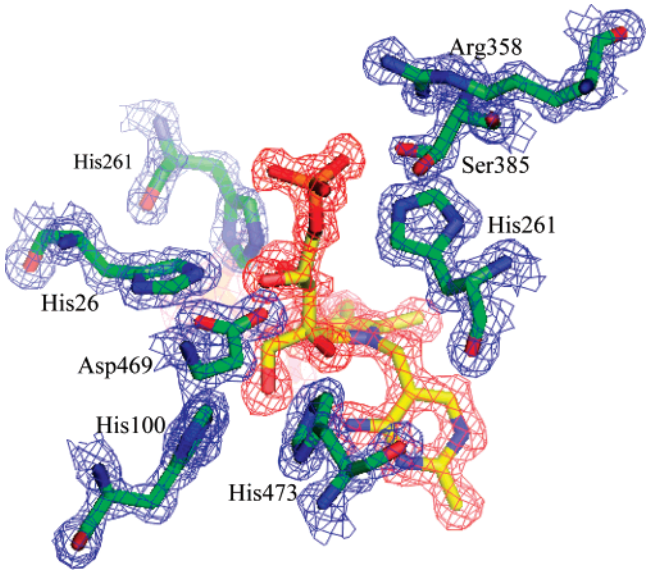

FIGURE 3: X-ray structure of the covalent X5P-ThDP intermediate trapped in the active site of TK from *E. coli* with selected amino acid side chains shown. The electron density of the side chains is contoured at 1.5σ and that of the intermediate at 1.3σ in a $2F_o - F_c$ map. For clarity, the electron density of the intermediate is depicted in red and that of the protein in blue. Please note that Ser385 adopts two alternative conformations.

difference to the reaction with the physiological donors X5P and F6P is most likely due to the fact that decarboxylation of the HPA-ThDP adduct can be considered to proceed in a quasi-irreversible manner, whereas cleavage of the X5P-ThDP and F6P-ThDP adducts is a reversible reaction. In line with that, the reaction of HPA with acceptors was found to proceed via a Ping−Pong mechanism (*31*).

X-ray Structure of the Covalent X5P-ThDP Adduct in TK. Crystals of TK were soaked with 25 mM X5P for approximately 20 s at 8 °C, and the structure of the resulting complex was solved by X-ray diffraction. The overall quality of both the diffraction data and the final model, judged by statistical parameters, is very good (Table 1): crystals diffracted to at least 1.47 Å, final values for R_{work} and R_{free} were 15.0% and 16.4%, respectively, and the overall B-factor from the Wilson plot was 9.7 Å^2.

The NMR-based intermediate analysis had indicated that the covalent X5P-ThDP adduct will be stabilized on the enzyme with an occupancy of 90% when X5P is added in saturating amounts. The crystallographic snapshot of TK after reaction with X5P reveals additional, very well-defined electron density close to the cofactor ThDP that can be interpreted as X5P being covalently bound to the cofactor (Figure 2) because (i) the shape of the C2 carbon of X5P is clearly tetrahedral, that is, sp^3 hybridized, and (ii) the interatomic distance between C2 of the sugar and C2 of ThDP is 1.5−1.6 Å, suggesting that the carbonyl addition of the sugar to ThDP's C2 had indeed taken place in the crystal. The electron density of the intermediate's C_α atom (C2 of X5P moiety) is not consistent with an sp^2-hybridized, planar trigonal C2 keto carbon of X5P, thus ruling out the possibility that the substrate is noncovalently held in a docking site. The electron density of all neighboring active site residues is also very well defined (Figure 3).

The covalent X5P-ThDP intermediate exhibits some very interesting structural features. At first, the C_α atom of X5P-ThDP (C2 of the sugar) is not in the ring plane of the thiazolium part of ThDP. As a consequence, there is a severe 25−30° out-of-plane distortion of the C2−Cα bond, which connects the sp^2-hybridized C2 of the aromatic thiazolium ring with the sp^3-hybridized C2 carbon of the sugar substrate (torsion angles: C5−S1−C2−Cα ≈ 25°, C4−N3−C2−Cα ≈ 30°). In order to ascertain that this observed out-of-plane distortion is not a crystallographic artifact due to incorrect data evaluation, we have conducted independent structural calculations and refinement cycles where the C2 atom of the sugar moiety has been forced into the ring plane by appropriate restraints. However, difference electron density maps clearly revealed that a model with a C2−Cα bond coplanar with thiazolium's ring plane is not consistent with the crystallographic data. The thiazolium ring of the intermediate is very slightly puckered; however, the interatomic distances (C2−N3, 1.35 Å; C4−C5, 1.38 Å) suggest a predominant aromatic character of the thiazolium ring. We have also carried out independent refinement cycles with in-plane restraints for the thiazolium ring atoms. The calculated structure of the intermediate deviates very marginally from that derived from structure calculation without in-plane restraints (Supporting Information, Figure S5). When implementing no in-plane restraints, the C2 ring atom is a few degrees out of the thiazolium ring plane. The apparent distortion of the C2−Cα bond implies considerable strain in the intermediate, which will be eventually relieved concomitantly with elimination of the product G3P and formation of the planar, unstrained DHEThDP enamine intermediate (*7*), thus providing a driving force for product elimination. Interestingly, similar findings have been described in structural studies on related ThDP enzymes that act on pyruvate. In pyruvate oxidase (POX) and pyruvate dehydrogenase (PDH), X-ray crystallographic snapshots of the pre-decarboxylation intermediate 2-α-lactyl-ThDP (LThDP, the covalent adduct of pyruvate and ThDP) and a phosphonate analogue of LThDP provided evidence for some

strain in these intermediates, varying from a 5−7° (POX) to 11° (PDH) out-of-plane distortion (*13*, *14*). We wish to note that a slight out-of-plane distortion of the C2−Cα bond has also been reported for post-decarboxylation intermediates trapped in the active sites of the human branched-chain α-ketoacid dehydrogenase multienzyme complex (*32*) and oxalyl-CoA decarboxylase (*33*) as opposed to the observation of planar enamine-type post-decarboxylation intermediates with an in-plane C2−Cα bond in POX (*13*), TK (*7*), and branched-chain α-ketoacid dehydrogenase from *Thermus thermophilus* (*34*). Thus, strain relief in the course of product elimination (sugar phosphates or CO_2) appears to be a driving force in most ThDP enzymes. Further studies will be required in the case of the human branched-chain α-ketoacid dehydrogenase multienzyme complex and oxalyl-CoA decarboxylase to substantiate that the observed electron density indeed corresponds to a carbanion-type post-decarboxylation intermediate (with a pyramidal Cα atom) as assigned rather than its conjugate acid, that is, the protonated hydroxyalkyl form, which would be tetrahedral.

The C2−C3 bond of the sugar moiety in the X5P-ThDP intermediate in TK, the bond that will be cleaved in the next step of catalysis, is almost perpendicularly directed relative to the aromatic thiazolium ring and has a bond length (1.54 Å) typical of C−C single bonds. This means that the observed electron density does not *a priori* require a relaxation of this bond length from the modeling restraint of 1.52 ± 0.02 Å, indicating that there is no specific structure-enforced destabilization of that bond already conserved in the intermediate. This is based on the good agreement of the model with the electron density; however, it should be considered that even at this high resolution, small changes in bond length might go undetected. The perpendicular orientation allows the positively charged thiazolium ring of ThDP to act as an optimal electron sink for the electron pair at DHEThDP's Cα generated upon elimination of G3P because facile conjugation of the formed electron pair with the thiazolium π-electrons is possible. Such a classic maximum overlap mechanism in thiamin enzymes had been predicted on the basis of theoretical considerations (*1*, *35*, *36*) and has already been shown to operate in enzymes catalyzing decarboxylation reactions (*13*, *14*). A direct comparison of the three-dimensional structures of the pre-decarboxylation intermediate *S*-LThDP in POX and X5P-ThDP in TK reveals that both intermediates adopt very similar conformations in the active site: the corresponding leaving groups (carboxylate in LThDP; G3P in TK) are positioned above the ring plane of the thiazolium part of the intermediates and the substrate-derived 2-hydroxyl group is in hydrogen-bonding distance to the 4′-amino group of the aminopyrimidine part of ThDP (Figure 4). Because of the more pronounced out-of-plane distortion in the X5P-ThDP intermediate, the distance between the intermediate's 2-hydroxyl group and the 4′-amino group is markedly longer in TK (3.2 Å) than that in LThDP trapped in POX (2.5 Å). In TK, the 1-hydroxyl group is also in hydrogen-bonding distance (3.1 Å) to the N4′ nitrogen of ThDP, whereas the corresponding methyl moiety of LThDP cannot form such an interaction.

A superposition of the X5P-ThDP intermediate with the structure of TK containing the unreacted cofactor (Figure 5A) demonstrates that there is some displacement of the

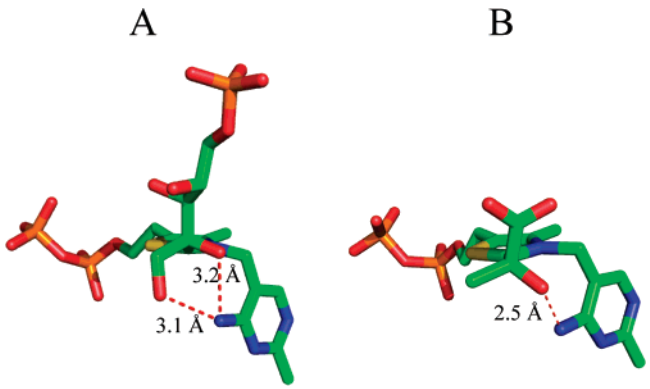

FIGURE 4: A structural comparison of the initial X5P-ThDP intermediate in TK (A) and the pre-decarboxylation intermediate 2-α-lactyl-ThDP (B) in POX (*13*) suggests a common substrate binding mode in thiamin enzymes with a perpendicular orientation of the leaving group relative to the aromatic thiazolium ring. The spatial proximity of the 4′-amino group of the aminopyrimidine part of ThDP to the substrate-derived carbonyl oxygen supports the proposed catalytic involvement of the aminopyrimidine ring as an intramolecular acid/base catalyst for substrate binding (*20*).

thiazolium ring and the ethyl part of the diphosphate anchor in the intermediate compared to the ground state, whereas the aminopyrimidine part, the diphosphate part of the cofactor, and the Ca^{2+} ion do not undergo structural rearrangements in the course of intermediate formation. An even more pronounced flexibility of the thiazolium ring has been reported for the related ThDP enzyme pyruvate/ferredoxin oxidoreductase (*37*), whereas there are only slight displacements of the thiazolium ring observable in POX at different intermediate stages (*13*).

The sugar-derived hydroxyl groups and phosphate moiety of the intermediate are firmly held in place through a network of hydrogen-bonding and electrostatic interactions with active site residues and the aminopyrimidine part of the cofactor (Figure 5B). The 1-hydroxyl and adjacent 2-hydroxyl group of the intermediate form hydrogen bonds with both the side chain of His473 and the 4′-amino group of the pyrimidine part of X5P-ThDP. In addition, the 1-hydroxyl group develops an interaction with His100. The 3-hydroxyl group interacts with the side chains of His261 and His26, whereas the 4-hydroxyl group forms two hydrogen bonds with the side chains of Asp469 and His26. Finally, the sugar-derived phosphate moiety of the intermediate is fixed through multiple interactions with the side chains of His461, Ser385, and Arg358. It is a remarkable fact, that no large structural rearrangements of active site residues occur in the course of intermediate formation (Figure 5B). This implies that the active site is poised for catalysis already in the ground state (absence of substrates). In total, the intermediate exhibits at least 11 well-defined hydrogen bonds and several electrostatic interactions. This large amount of productive interactions plus the nonobservance of structural changes suggest that the binding energy ΔG_B of the substrate may at least partially compensate for the energy required to form the high-energy strained intermediate. In this way, the binding energy of the substrate is chemically channeled and accumulated in the strained intermediate. The multiple interactions of active site residues with the substrate apparently fix it in a rigid manner close to the reactive thiazolium part of ThDP. The reactive C2 carbanion of the cofactor may then spontaneously add to the 2-keto carbon of the substrate because the carbonyl

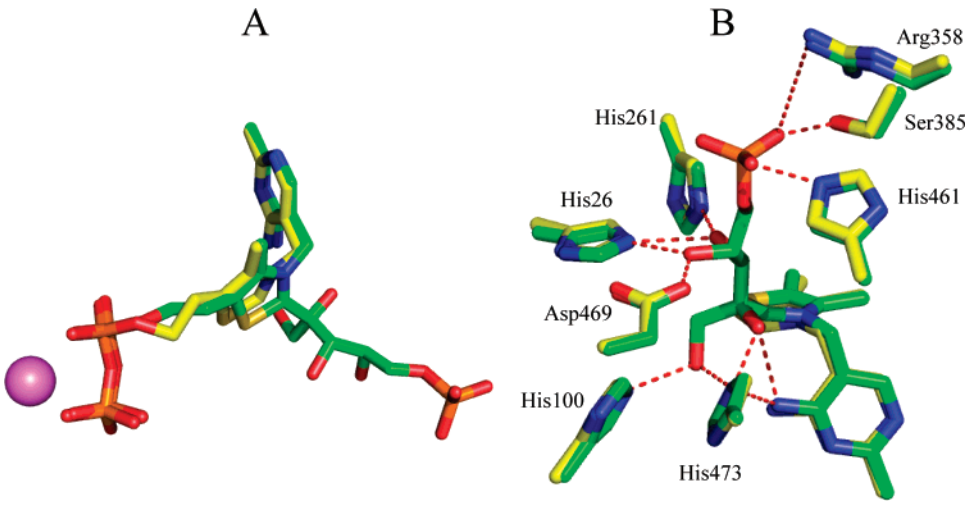

FIGURE 5: Superposition of the active site of TK with the bound X5P-ThDP reaction intermediate (green) and that of the unreacted enzyme in the ground state (yellow) showing either only ThDP versus X5P-ThDP (A) or cofactor and intermediate plus selected amino acid residues (B). Superposition was accomplished after least-squares fitting of all protein atoms using the program Coot. In (B), the diphosphate anchors of ThDP and X5P-ThDP were deliberately omitted for the sake of clarity.

addition of substrate to C2 can be considered a very exergonic reaction. The cofactor itself is also held in tight interactions with active site groups and thus may not undergo large structural changes, which could avoid strain in the intermediate. Nevertheless, the thiazolium moiety of the cofactor moves slightly toward the substrate (Figure 5A). Paraphrased, the binding energy of substrate/cofactor plus the enthalpic gain in energy of the carbonyl addition appear to conjointly enforce the formation of a high-energy, strained intermediate. Contrary to what has been suggested for the observed strain in a pre-decarboxylation intermediate analogue in PDH (*14*), a repulsive interaction between the aminopyrimidine N4′ and Cα-OH is less likely to account for the observed out-of-plane distortion in TK (see DFT studies in the next section). We rather suggest that the built-in structural complementarity of enzyme and substrate provides a major driving force for catalysis, that is, the formation of the strained intermediate. In order to test this hypothesis, we have generated the TK double variant His26Ala/His261Ala in which three hydrogen-bonding interactions between the active site and the 3-hydroxyl and 4-hydroxyl groups of the intermediate cannot be formed when compared to the wild-type enzyme. Under identical reaction conditions, as established for the wild-type enzyme and substrate saturation (25 mM), the fraction of the covalent donor−ThDP adduct under equilibrium conditions is significantly smaller (Supporting Information, Figure S6) as observed for wild-type TK (see Figure 1B). This result indicates that the productive interactions of active-site side chains are presumably a key factor for mediating the formation of the covalent strained intermediate. As the donor substrates' apparent K_M values are virtually unchanged in the variant when compared to those of the wild-type enzyme, the low occupancy with covalent donor−ThDP adduct in equilibrium should not result from a diminished bimolecular binding of the substrate to form the Michaelis complex but rather from a higher kinetic barrier for covalent bond formation. We wish to note, however, that additional detailed kinetic, thermodynamic, and structural studies involving protein variants and substrate analogues lacking certain OH groups will be required to prove our hypothesis that

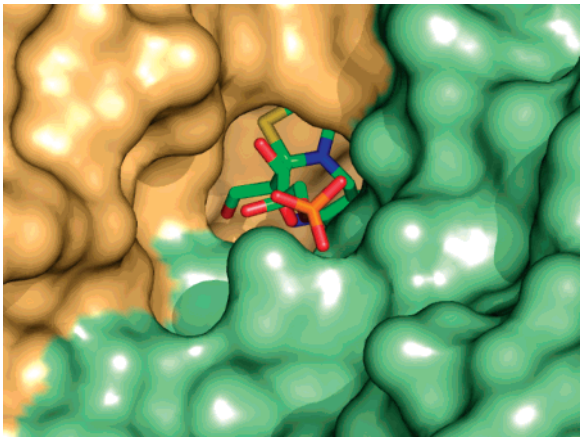

FIGURE 6: Surface view of TK viewed down the substrate channel with the enzyme-bound X5P-ThDP intermediate bound at the dimer interface. The subunits of the dimer are colored individually.

productive hydrogen-bonding interactions help to distort the covalent donor−ThDP intermediate. Further quantitative studies on the double variant and various other active site variants of *Ec*TK are in progress in our laboratories.

A surface view of the enzyme (viewed down the substrate channel) shows that the G3P leaving group is directed outside the active site. After C2−C3 bond cleavage in the X5P-ThDP intermediate, the resultant product G3P can diffuse out of the active site without steric hindrance (Figure 6). We could observe the intermediate in both active sites of the TK dimer with similar high occupancy arguing against a half-of-the-sites mechanism shown to operate in PDH enzymes (*38*, *39*).

DFT Studies on X5P−Thiamin and X5P−Thiazolium Models. The apparent out-of-plane distortion of the C2−Cα bond in the X5P-ThDP intermediate raises several mechanistic questions. How much energy is required to distort the intermediate? Which interactions of the intermediate at the active site provide that energy? To answer these questions, we have conducted DFT calculations on simplified X5P−thiamin and X5P−thiazolium models. At first, the total energy of X5P−thiamin was calculated without any further optimization (single-point calculation) for (i) the experimentally observed, strained conformation of the adduct and (ii)

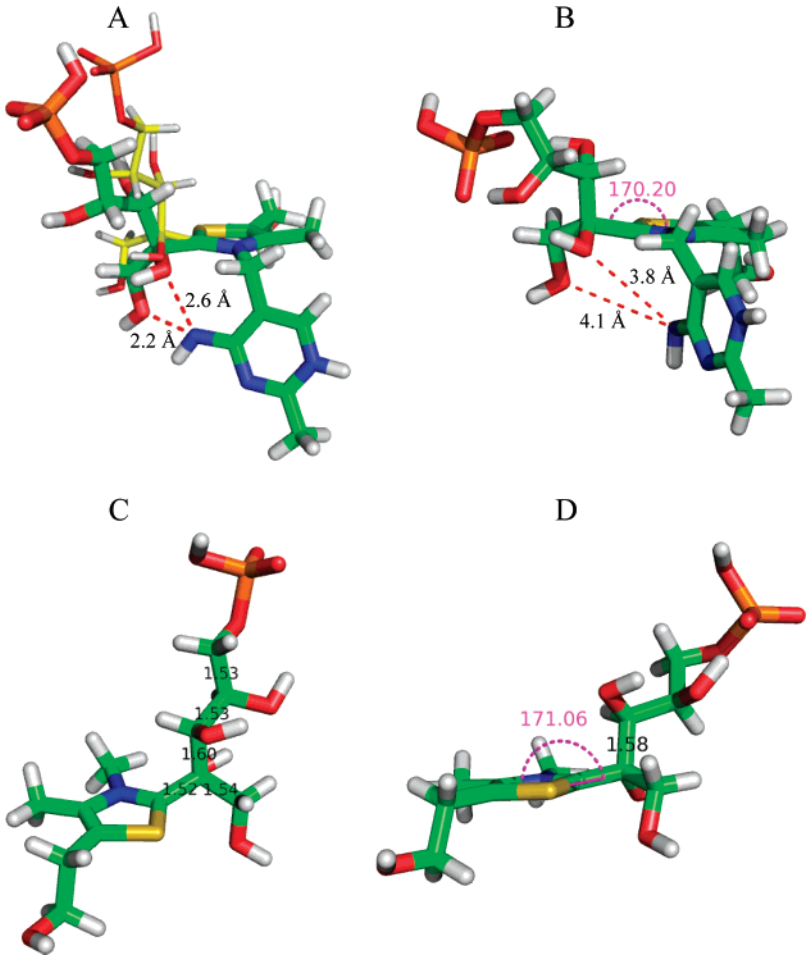

FIGURE 7: DFT studies on X5P−thiamin and X5P-thiazolium models. (A) Structural comparison of X5P−thiamin in the experimentally observed strained conformation (yellow) and in a conformation where the C2−Cα bond is in-plane (green, torsion angle C5−S1−C2−Cα = 180°). For the latter form, the interatomic distances between N4′ and O1/O2 of the sugar moiety are indicated. (B) Structure of X5P−thiamin after full optimization. The calculated torsion angle C5−S1−C2−Cα is indicated. (C) Structure of X5P-thiazolium after partial optimization (torsion angle C5−S1−C2−Cα and those of the sugar moiety were retained as in the X-ray structure). The C−C bond lengths of the sugar main chain are indicated. (D) Structure of X5P-thiazolium after full optimization. The calculated C5−S1−C2−Cα torsion angle and the C2−C3 bond length are indicated.

a conformation in which the C2−Cα bond is relaxed, that is, in-plane (torsion angle C5−S1−C2−Cα = 180°). Remarkably, the total energy of unstrained X5P−thiamin is 75 kJ/mol *higher* than that of the experimentally determined strained structure. As shown in Figure 7A, if the C2−Cα bond of X5P−thiamin was to be in-plane, the sugar-derived 1-OH and 2-OH groups would be in closer contact with the 4′-imino nitrogen of the iminopyrimidine moiety as compared to the strained structure. Whereas N4′ and O2 of the sugar would be in a reasonable distance (2.6 Å) for hydrogen bonding, the very short interatomic distance between N4′ and O1 (2.2 Å) suggests a strong repulsive interaction, which presumably accounts for the higher energy of the in-plane conformation.

Next, a fully optimized X5P−thiamin model (Figure 7B) was calculated starting both from out-of-plane and from in-plane structures. In the resultant optimized structure (E_T = 517 kJ/mol lower than that of the experimentally observed strained structure), the relative spatial orientations of the thiazolium and aminopyrimidine rings, characterized by the torsional angles Φ_T (C5′-C3,5′−N3−C2) and Φ_P (N3−C3,5′−C5′-C4′), have changed from *the V* conformation (Φ_T = 100°, Φ_P = −65°) adopted at the active site to a conformation in which the aminopyrimidine ring is slightly rotated versus the thiazolium ring (Φ_T = 122°, Φ_P = −41°). Consequently, there would be no repulsive interactions between the sugar moiety and the 4′-imino group. The sugar chain adopts a slightly different conformation and develops an intramolecular hydrogen-bond interaction between the phosphate part and 4-OH. The scissile C2−C3 bond remains in a perpendicular orientation relative to the thiazolium ring. Most remarkably, the C2−Cα bond deviates from planarity even after full optimization, although to a lesser extent (≈ 10°) than in the X-ray structure (≈ 25−30°). This result suggests that not only repulsive interactions of the sugar moiety with the 4′-imino group of the intermediate in the *V* conformation enforce the apparent out-of-plane distortion. To study the energetics of the sugar−cofactor adduct without the aminopyrimidine, DFT calculations on X5P−thiazolium models were carried out with partial and full optimization. For partial optimization (Figure 7C), the torsional angles of the sugar chain and that of the C5−S1−C2−Cα bond were retained as in the X-ray structure by appropriate constraints to enforce an overall conformation, which is most likely and relevant for catalysis at the active site. An analysis of the carbon−carbon bond length of the sugar chain shows that the scissile C2−C3 bond (1.60 Å) is selectively weakened in that conformation. Full optimization of X5P−thiazolium

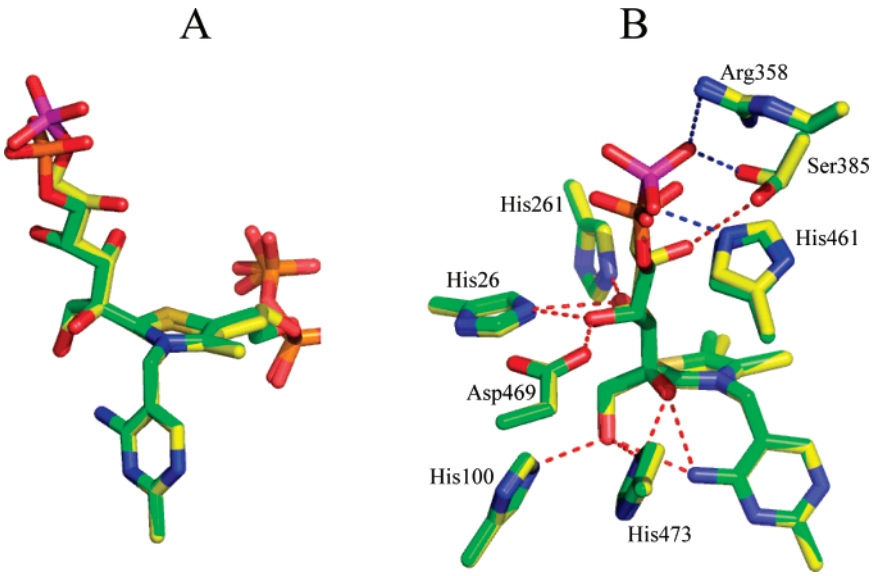

FIGURE 8: (A) Superposition of the X5P-ThDP (green) and F6P-ThDP (yellow) intermediates in the active site of TK from *E. coli*. For clarity, the phosphorus atom of the F6P-ThDP intermediate is colored in magenta. Both intermediates adopt very similar extended conformations with an apparent out-of-plane distortion of the C2−Cα bond (see text) formed between C2 of ThDP and C2 of the sugar. The corresponding sugar-derived oxygen and carbon atoms of the intermediates occupy virtually identical positions. As a result of the different chain lengths of the alternative substrates X5P (5-carbon) and F6P (6-carbon), the position of the intermediate's phosphate moiety is slightly different in the two intermediates. (B) Interactions of the X5P-ThDP and F6P-ThDP intermediates in the active site. Hydrogen-bonding interactions of substrate-derived hydroxyl groups are indicated in red, and the specific interactions of the phosphate moiety of the F6P-ThDP intermediate are shown in blue. Please note that the 5-hydroxyl group of the F6P-ThDP intermediate forms an additional hydrogen bond to Ser385. For clarity, the diphosphate anchor of the intermediates is not shown in this panel.

(Figure 7D) yields a slightly different structure (E_T = 91 kJ/mol lower than that of the partially optimized structure) with a conformation of the sugar moiety similar to that observed for fully optimized X5P−thiamin. More intriguing, the C2−Cα bond is still out-of-plane by approximately 9°, and the sugar's C2−C3 bond (1.58 Å) is longer than a typical C−C single bond (1.53 Å).

On the basis of the DFT studies, it may be concluded that the intrinsic electronic and chemical characteristics of the thiazolium ring enforce strain in the tetrahedral X5P−cofactor adduct. As the out-of-plane distortion of the C2−Cα bond in a X5P−thiazolium model (9°) is less pronounced than observed in the X-ray structure (25−30°), additional factors are required for further distortion, such as productive interactions of the sugar's OH-groups with active site residues and intramolecular repulsion between the sugar moiety and the 4′-aminopyrimidine, as also suggested for tetrahedral intermediates in PDH by Furey and Jordan (*14*).

X-ray Structure of the Covalent F6P-ThDP Adduct in TK. The addition of the alternative donor ketose F6P at saturating amounts (25 mM) to TK results in the formation of the covalent sugar adduct F6P-ThDP in the active site with an occupancy of approximately 75% active sites total as detected by NMR spectroscopy (see Figure 1B). An X-ray crystallographic snapshot of TK after reaction with F6P for 20 s at 1.65 Å resolution reveals the defined electron density of the covalent F6P-ThDP intermediate, similar to that observed for the X5P-ThDP intermediate. A superposition of both intermediates shows that the sugar moiety of the F6P-ThDP intermediate adopts a similar extended, perpendicular oriented conformation as the corresponding part in the X5P-ThDP intermediate (Figure 8). There is also a marked out-of-plane distortion in the C2−Cα bond in the intermediate of approximately 25−30° relative to the thiazolium ring. The sugar-derived carbon chain and corresponding oxygen atoms of both intermediates occupy almost identical positions in the active site (Figure 8A). The phosphate moiety of the F6P-ThDP intermediate binds in a manner slightly different from that of X5P-ThDP as a result of the longer carbon chain in the 6-carbon F6P. Consequently, the phosphate accommodates closer to the side chains of Arg358, Ser385, and His461 (Figure 8B). The additional 5-hydroxyl group in the F6P-ThDP intermediate develops a new interaction with the side chain of Ser385. All other hydrogen-bonding interactions of the intermediate's sugar part with active-site side chains and the aminopyrimidine ring are conserved with respect to the X5P-ThDP intermediate. Also, there are no apparent structural differences in the active site architecture when either the X5P-ThDP or F6P-ThDP intermediate is present, suggesting that the active site is predestined to deal with substrates of different chain length. The conserved interactions of the sugar-derived hydroxyl groups 1−4 in both intermediates appear to contribute the major part of substrate-binding energy, which finally enforces, conjointly with the intrinsic features of the cofactor (see DFT studies), the apparent out-of-plane distortion. The slightly different interactions with the phosphate moiety and inherent different binding energies are not as decisive as the interaction with the hydroxyl groups. However, nonphosphorylated sugar substrates are very poor substrates (*8*) demonstrating that the interactions of the phosphate part contributes to the overall binding energy of the substrate.

X-ray Structure of the Acceptor R5P Trapped in the Active Site of TK. ITC experiments demonstrate that the acceptor aldose R5P binds to TK even in the absence of donor substrates or derived intermediates with an apparent dissociation constant of approximately 700 μM (Supporting Information, Figure S7). As the ITC data fit to a one site binding model with a stoichiometry of 1 molecule R5P per

active site, this implies that R5P binds to both active sites with similar affinity.

After soaking *holo*-TK crystals with saturating amounts of R5P (25 mM) for 1 min at 8 °C and determining the X-ray structure, additional electron density can be observed in both active sites, which we attribute to R5P held in a docking site. The electron density assigned to R5P cannot be interpreted as unambigously as in the case of the covalent X5P-ThDP and F6P-ThDP intermediates and cannot be explained when only one conformer of R5P is considered to account for the density (Figure 9). We rather suggest that the density is attributable to at least two different conformers of R5P. The density of R5P in both active sites is slightly different, whereas there are no structural differences observable for the two subunits of the dimer. In one active site (upper panel in Figure 9), the density can be reasonably explained when R5P exists as a ring-closed β-D-furanose in C2-*exo* conformation, although there is no defined density observable for the O1 hydroxyl group of the sugar. Notably, the C2-*exo* structure of R5P appears to be slightly strained as O, C1, C3, and C4 are out-of-plane by approximately 10−14°. In the other active site (lower panel in Figure 9), the electron density of the substrate is less defined and suggests that R5P is present both in a ring-closed form similar to the other active site but with even more strain and presumably in an extended acyclic *aldo* form. Whereas the phosphate moiety of R5P in the latter active site is well defined, there appears to be some flexibility/alternative conformations for the remaining part of R5P such as the C1 *aldo* group. After careful inspection of the electron density maps of the active site (both omit maps and maps after refinement), we believe that an open form has to be taken into account because there is additional electron density in the omit map, which we assign to the C1 *aldo* oxygen of an extended acyclic form, and that is clearly different from those of all active-site waters. Also, when only a cyclic structure of R5P is taken into account for model building and structure refinement, the difference electron density maps suggest that some fraction R5P in the active sites is present in an open form (Figure 10). We have to admit, however, that an ultimate assignment cannot be made on the basis of current data. If indeed an acyclic form of R5P can be stabilized on the enzyme's active site as modeled, it would be in a very favorable position to attack the DHEThDP enamine intermediate (Figure 11). We have modeled the planar enamine into the structure of *E. coli* TK using the structural data of the intermediate obtained on the yeast enzyme (*7*). The distance of the C1 *aldo* carbon of R5P would then be in close proximity (1.6 Å) to the Cα atom of the enamine and in a very favorable angle of 112° relative to the C2−Cα bond. The next reaction step, the bond formation between C1 *aldo* of R5P and Cα of the enamine would only require rehybridization of both carbons from sp^2 to sp^3 without structural rearrangements. Model studies and theoretical considerations have predicted such an orientation of the reactants, which has been termed the Bürgi−Dunitz trajectory of carbonyl addition/elimination reactions (*40*).

As shown in Figure 9, R5P is firmly held in place in the active site through multiple interactions with active-site residues. In the ring-closed β-D-furanose form, the hydroxyl groups of the sugar form an array of hydrogen-bonding interactions with His261, His26, and Asp469. The phosphate

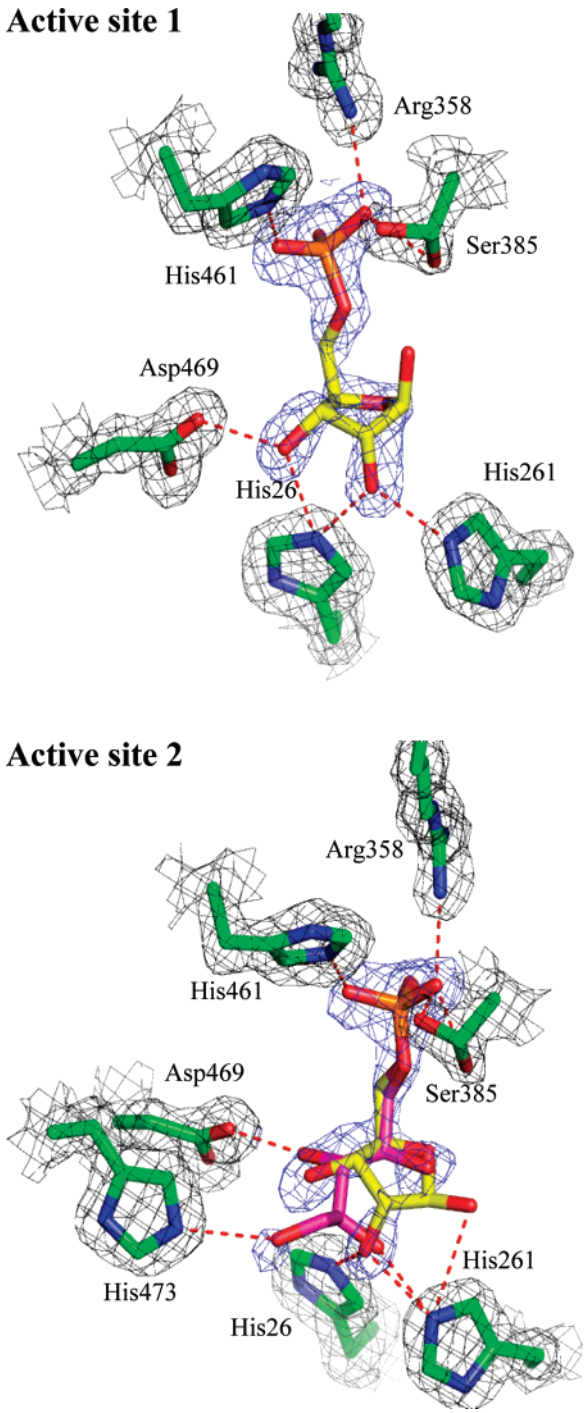

FIGURE 9: X-ray structure of the acceptor aldose R5P trapped in the active sites of bacterial TK with selected amino acid side chains shown. The two different active sites of the dimer are shown in separate panels. The electron density of R5P is contoured at 1σ in a $F_o - F_c$ omit map prior to the inclusion of the sugar atoms in the refinement, and that of proximal active site residues is contoured at 1σ in a $2F_o - F_c$ map. For clarity, the different conformers of R5P in active site 2 (lower panel) are colored individually (open form in pink; closed form in yellow). Please note that Ser385 adopts two alternative conformations.

moiety accommodates in close proximity to Ser385, His461, and Arg358. If indeed an open form of R5P can be formed in the active site as we have modeled (see above), its 1-*aldo* group would develop an additional interaction with His473 (lower panel in Figure 9). This interaction presumably helps to stabilize the reactive open *aldo* form in the active site. As outlined before, in free solution, there is only a small

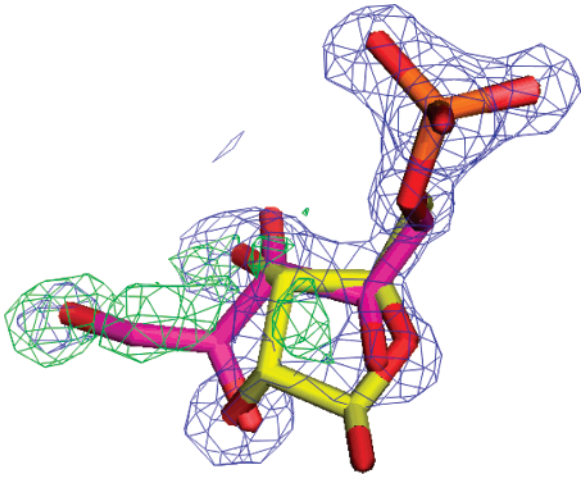

FIGURE 10: X-ray structure of R5P bound in the active site of TK from *E. coli*. The electron density of cyclic R5P after refinement is shown at 1σ in a $2F_o - F_c$ map. The difference electron density $F_o - F_c$ maps reveal positive electron density (green, contoured at 3.5σ) in the substrate binding pocket, which we assign to a linear form of R5P.

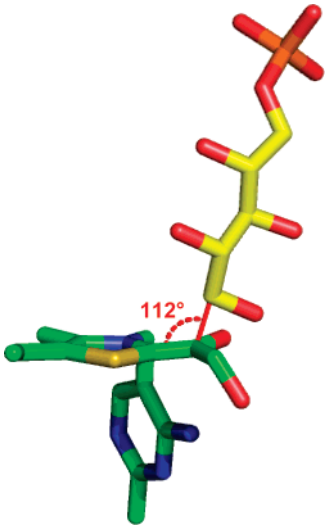

FIGURE 11: Orientation of R5P in an acyclic conformation relative to the planar enamine-type DHEThDP intermediate, the latter modeled into the active site of bacterial TK according to ref *7*. The C1 *aldo* carbon of R5P would be in a favorable position to attack the Cα of the enamine intermediate exhibiting an interatomic distance of approximately 1.6 Å and an angle of 112° relative to the C2−Cα bond. This orientation would be consistent with the predicted least-motion mechanism of carbonyl additions according to the Bürgi−Dunitz trajectory.

amount of acyclic R5P (0.05−0.10%) thermodynamically stabilized. We propose that the productive interaction of the C1 *aldo* oxygen with the active site provides in addition to the strain exerted on the envelope ring structure of R5P a driving force for the stabilization of the open form in a near-attack conformation with respect to the DHEThDP enamine intermediate. The structural transition from the ring-closed β-D-furanose form to the open acyclic *aldo* form (Figure 9, lower panel) would only require a rotation of the C2−C3 bond of R5P of approximately 180° such that the C1 *aldo* group would flip on the opposite side compared to the ring-closed form. All other atoms would only undergo minor structural rearrangments. Consequently, most of the hydrogen bonds and electrostatic interactions formed between the sugar and side chains would be conserved except for the interaction

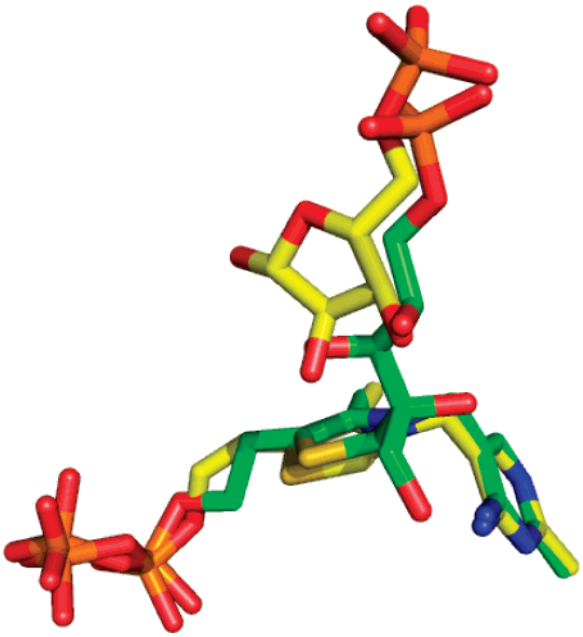

FIGURE 12: Relative spatial orientation of R5P in a ring-closed form (yellow), held in a docking site close to ThDP (yellow), and the covalent X5P-ThDP intermediate (green), both trapped independently in the active site of TK after superimposition of all protein atoms.

of the C1 oxygen, which interacts with His261 in the ring-closed form and with His473 in the open *aldo* form. No large structural changes occur in the course of R5P binding when compared to the ground state of the enzyme as also observed for the covalent addition of the donor substrates (data not shown).

NMR studies (see the first part of the Results and Discussion section) had indicated that the covalent donor−ThDP adduct (X5P-ThDP and F6P-ThDP) is stabilized on the enzyme in the absence of an acceptor. Although the DHEThDP enamine is not (substrate X5P) or barely (substrate F6P) detectable by ^{1}H NMR, this intermediate is, according to our NMR and steady-state kinetic studies, in rapid equilibrium with the corresponding donor−cofactor adduct. A structural comparison of TK containing covalently bound donor X5P and noncovalently bound acceptor R5P reveals that the binding site of the acceptor partially overlaps with that of the covalent donor−cofactor intermediate (Figure 12). In the ring-closed form, the 2- and 3-hydroxyl groups of R5P occupy positions similar to those of the 3- and 4-hydroxyl groups of the X5P-ThDP intermediate, whereas the R5P carbon ring atoms would be bound alongside the carbon chain of X5P-ThDP. The phosphate moiety of R5P binds in a manner slightly different from that of X5P-ThDP. Although it is conceivable that R5P and X5P cannot be bound at the same time in the active site as shown in Figure 12, the almost identical binding sites suggest that the products of donor cleavage (G3P and E4P) and R5P compete for the same hydrogen-bonding and electrostatic interactions and eventual carboligation to the DHEThDP enamine in two competing equilibria. A likewise competition can be expected to exist for donor and acceptor binding being in line with our kinetic steady-state studies, which clearly indicated a direct competition between donor X5P and acceptor R5P (Supporting Information, Figure S3).

To study the lifetime of the elusive DHEThDP enamine at the true steady state (Supporting Information, Figure S8), we have conducted NMR-based intermediate studies in the presence of donor (either X5P or F6P) *and* acceptor R5P and compared these results with those obtained in the presence of donor only (Figure 1B). Our studies reveal that the fraction of the covalent donor−ThDP adduct/total intermediates decreases after the addition of R5P to TK with X5P-ThDP or F6P-ThDP stabilized on the active site beforehand, that is, binding of the acceptor slightly shifts the intermediate distribution. Intriguingly, we were unable to detect DHEThDP or other covalent intermediates such as S7P-ThDP (the adduct formed between ThDP and the product S7P). The large fraction of unreacted cofactor and covalent donor−ThDP adduct implies that the formation and decay of the covalent donor−cofactor intermediate (steps 1 and 2 in Figure 1A) are partially rate-limiting for TK catalysis at steady state when donor and acceptor are present at saturating amounts. By contrast, the covalent ligation of acceptor to the DHEThDP enamine and product release (steps 3 and 4 in Figure 1A) are not rate-limiting and must be significantly faster than steps 1 and 2.

CONCLUSIONS

The mechanisms by which enzymes achieve their awesome rate enhancements compared to those of the corresponding nonenzymatic reactions have been the subject of intense biochemical studies and are still under debate (*41*, *42*). While there is now compelling experimental evidence for how the chemical catalysis (covalent catalysis and acid/base catalysis) provided by enzymes contributes to rate acceleration, there is less experimental data available that demonstrate the beneficial use of substrate-binding energy for chemically difficult reactions. With the advent of the seminal transition state theory, Emil Fischer's suggestion of enzyme−substrate complementarity in terms of a lock and key model had to be modified, and it is now commonly accepted that enzymes exhibit preferential binding of the transition state rather than of the substrate or product. Computational studies on different enzymes have suggested that highly specific steric and electronic interactions of the enzyme and substrate may select for subpopulations of substrate conformers aligning them in favorable orientation and distance to active site catalysts, referred to as near attack conformers (*43*, *44*). Also, as predicted by the famous Circe effect theory from W. P. Jencks (*45*), there have been instances where productive interactions of the enzyme with some nonreacting part of the substrate lure the latter into the active site enforcing an orientation in which the substrate's reactive part is exposed to electrostatic or steric stress as in the case of OMPDase (*46*).

Here, our studies on the ThDP enzyme TK covering both NMR-based kinetics as well as X-ray crystallographic snapshots along the reaction trajectory give instructive insights into general principles of enzymatic catalysis and demonstrate how an enzyme may take advantage of substrate-binding energy conjointly with the intrinsic electronic properties of its cofactor to form high-energy strained intermediates or strained substrates.

In the reaction catalyzed by the thiamin enzyme TK, the donor ketoses X5P or F6P will first covalently add to the enzyme-bound cofactor ThDP yielding a tetrahedral cofactor−substrate intermediate that is sufficiently stable under equilibrium conditions for a structural analysis. The X-ray structures of TK in covalent complex with X5P/F6P revealed that there is significant strain in the intermediates, as the C2−Cα bond, which connects the sp^2 carbon 2 of the cofactor's thiazolium ring with the sp^3 carbon 2 of the sugar substrate, is not coplanar with the thiazolium ring plane. The out-of-plane distortion of this bond by 25−30° implies considerable strain in the intermediate. It is conceivable that this strain is a driving force for product elimination because the strain will be eventually relieved upon formation of the planar, unstrained enamine intermediate. A structural comparison of the enzyme in the ground state and in the intermediate state shows that there are with the exception of some slight displacement of the cofactor itself no detectable structural rearrangements occurring in the course of intermediate formation, that is, the enzyme is poised for catalysis already in the ground state. The sugar-derived hydroxyl groups and phosphate moiety of the intermediates form numerous productive hydrogen-bonding and electrostatic interactions with a cluster of His side chains and conserved Asp, Ser, and Arg residues. All these interactions help to fix the substrate in a way that its carbonyl carbon is placed in striking distance to the highly reactive C2 carbanion of the ThDP cofactor. Theoretical considerations suggest that the subsequent covalent addition of the substrate to the high-energy ThDP C2 carbanion gains a lot of enthalpic energy (*3*), which together with the substrate's binding energy is channeled into the formation of a strained, high-energy intermediate. Our DFT calculations on X5P−thiamin models have shown that the intermediate with the experimentally observed out-of-plane distortion is energetically favorable by 75 kJ/mol when compared to a model with a coplanar C2−Cα bond. In the latter form, there would be a strong intramolecular repulsion between the 1-hydroxyl group of the sugar moiety and the 4′-imino group of the intermediate. However, the repulsion between 4′-amino/1′,4′-imino and 1-OH cannot solely be responsible for the apparent strain as a full optimization of X5P-thiazolium models (without the aminopyrimidine moiety) also resulted in C2−Cα bond that is out-of-plane by 9°. Hence, it seems to be an intrinsic feature of the thiazolium ring to enforce the strain of tetrahedral intermediates and a perpendicular orientation of the corresponding leaving group. Further DFT studies on related tetrahedral intermediates such as LThDP support this suggestion (Friedemann, R., and Tittmann, K., manuscript in preparation).

Our structural studies on the noncovalent complex of TK with the acceptor aldose R5P showed that contrary to free solutions R5P can be bound/stabilized in an acyclic, extended conformer with the C1 *aldo* function held close to the DHEThDP enamine intermediate in an almost perfect orientation for bond formation occurring in the next step of catalysis. Thus, TK constitutes an example for the stabilization of near-attack conformers of a substrate in the active-site environment. The driving forces for the formation of the open sugar form are probably (i) destabilization of the ring-closed conformer by strain (induced by interactions with the active site) and (ii) productive interactions of the C1 *aldo* group of linear R5P with active site residues (e.g., His473).

Finally, we wish to note that the reactive DHEThDP enamine is a very short-lived intermediate in *Ec*TK catalysis. Under steady-state conditions, only the unreacted cofactor and the tetrahedral donor-ThDP adduct can be detected, implying the formation and decay of that initial intermediate to be rate-determining for overall catalysis as opposed to carboligation of acceptor and the DHEThDP enamine, which escapes detection under the conditions used. The small population of DHEThDP during turnover guarantees that undesired side reactions of the highly reactive enamine, such as oxygenation or protonation of Cα and subsequent elimination of glycolaldehyde, can be minimized.

ACKNOWLEDGMENT

We gratefully acknowledge enlightening discussions on the chemical interpretation of the structural studies on intermediates in TK with Richard Schowen, Ron Kluger, Frank Jordan, Peter Guthrie, and Jik Chin. We thank Georg Sprenger for providing the plasmid pGSJ427 encoding TKA. We gratefully acknowledge access to synchrotron radiation beamline BW7B at the European Molecular Biology Laboratory outstation, Deutsches Elektronen-Synchrotron, Hamburg, Germany. We would also like to thank Milton T. Stubbs for helpful discussions and generous access to the in-house X-ray facilities of his group.

SUPPORTING INFORMATION AVAILABLE

Further 1H NMR-based intermediate studies on (i) *Ec*TK wild-type (donor-only reaction and at the true steady state) and (ii) double variant H26A/H261A (donor-only reaction); analysis of the enzyme-catalyzed conversion of the artificial donor substrate β-hydroxypyruvate by stopped-flow and chemical quenched-flow/NMR kinetics; and ITC studies of R5P binding. This material is available free of charge via the Internet at http://pubs.acs.org.

REFERENCES

1. Kluger, R. (1987) Thiamin diphosphate: a mechanistic update on enzymic and nonenzymic catalysis of decarboxylation, *Chem. Rev. 87*, 863−876.
2. Schellenberger, A. (1998) Sixty years of thiamin diphosphate biochemistry, *Biochim. Biophys. Acta 1385*, 177−186.
3. Schowen, R. L. (1998) Thiamin Enzymes. In *Comprehensive Biological Catalysis* (Sinnot, M., Ed.) Vol. 2, pp 217−266, Academic Press, London.
4. Jordan, F. (2003) Current mechanistic understanding of thiamin diphosphate-dependent enzymatic reactions, *Nat. Prod. Rep. 20*, 184−201.
5. Schneider, G., and Lindqvist, Y. (1998) Crystallography and mutagenesis of transketolase: mechanistic implications for enzymatic thiamin catalysis, *Biochim. Biophys Acta 1385*, 387−398.
6. Schenk, G., Duggleby, R. G., and Nixon, P. F. (1998) Properties and functions of the thiamin diphosphate dependent enzyme transketolase, *Int. J. Biochem. Cell Biol. 30*, 1297−1318.
7. Fiedler, E., Thorell, S., Sandalova, T., Golbik, R., König, S., and Schneider, G. (2002) Snapshot of a key intermediate in enzymatic thiamin catalysis: crystal structure of the alpha-carbanion of (alpha,beta-dihydroxyethyl)-thiamin diphosphate in the active site of transketolase from Saccharomyces cerevisiae, *Proc. Natl. Acad. Sci. U.S.A. 99*, 591−595.
8. Nilsson, U., Meshalkina, L., Lindqvist, Y., and Schneider, G. (1997) Examination of substrate binding in thiamin diphosphate-dependent transketolase by protein crystallography and site-directed mutagenesis, *J. Biol. Chem. 272*, 1864−1869.
9. Wikner, C., Meshalkina, L., Nilsson, U., Nikkola, M., Lindqvist, Y., Sundstrom, M., and Schneider, G. (1994) Analysis of an invariant cofactor-protein interaction in thiamin diphosphate-dependent enzymes by site-directed mutagenesis. Glutamic acid 418 in transketolase is essential for catalysis, *J. Biol. Chem. 269*, 32144−32150.
10. Wikner, C., Meshalkina, L., Nilsson, U., Backstrom, S., Lindqvist, Y., and Schneider, G. (1995) His103 in yeast transketolase is required for substrate recognition and catalysis, *Eur. J. Biochem. 233*, 750−755.
11. Wikner, C., Nilsson, U., Meshalkina, L., Udekwu, C., Lindqvist, Y., and Schneider, G. (1997) Identification of catalytically important residues in yeast transketolase, *Biochemistry 36*, 15643−15649.
12. Nilsson, U., Hecquet, L., Gefflaut, T., Guerard, C., and Schneider, G. (1998) Asp477 is a determinant of the enantioselectivity in yeast transketolase, *FEBS Lett. 424*, 49−52.
13. Wille, G., Meyer, D., Steinmetz, A., Hinze, E., Golbik, R., and Tittmann, K. (2006) The catalytic cycle of a thiamin diphosphate enzyme examined by cryocrystallography, *Nat. Chem. Biol. 2*, 324−328.
14. Arjunan, P., Sax, M., Brunskill, A., Chandrasekhar, K., Nemeria, N., Zhang, S., Jordan, F., and Furey, W. (2006) A thiamin-bound, pre-decarboxylation reaction intermediate analogue in the pyruvate dehydrogenase E1 subunit induces large scale disorder-to-order transformations in the enzyme and reveals novel structural features in the covalently bound adduct, *J. Biol. Chem. 281*, 15296−15303.
15. Angyal, S. J. (1969) The composition and conformation of sugars in solution, *Angew. Chem., Int. Ed. Engl. 8*, 157−226.
16. Hayward, L. D., and Angyal, S. J. (1977) A symmetry rule for the circular dichroism of reducing sugars and the proportion of carbonyl forms in aqueous solutions thereof, *Carbohydr. Res. 53*, 13−20.
17. Wu, J., Serianni, A. S., and Vuorinen, T. (1990) Furanose ring anomerization: kinetic and thermodynamic studies of the D-2-pentuloses by 13C-n.m.r. spectroscopy, *Carbohydr. Res. 206*, 1−12.
18. Swenson, C. A., and Barker, R. (1971) Proportion of Keto and Aldehydo Forms in Solutions of Sugars and Sugar Phosphates, *Biochemistry 10*, 3151−3154.
19. Sprenger, G. A., Schörken, U., Sprenger, G., and Sahm, H. (1995) Transketolase A of Escherichia coli K12. Purification and properties of the enzyme from recombinant strains, *Eur. J. Biochem. 230*, 525−532.
20. Tittmann, K., Golbik, R., Uhlemann, K., Khailova, L., Schneider, G., Patel, M., Jordan, F., Chipman, D. M., Duggleby, R. G., and Hübner, G. (2003) NMR analysis of covalent intermediates in thiamin diphosphate enzymes, *Biochemistry 42*, 7885−7891.
21. Frisch, M. J., Trucks, G. W., Schlegel, H. B., Scuseria, G. E., Robb, M. A., Cheeseman, J. R., Zakrzewski, V. G., Montgomery, J. A., Jr., Stratmann, R. E., Burant, J. C., Dapprich, S., Millam, J. M., Daniels, A. D., Kudin, K. N., Strain, M. C., Farkas, O., Tomasi, J., Barone, V., Cossi, M., Cammi, R., Mennucci, B., Pomelli, C., Adamo, C., Clifford, S., Ochterski, J., Petersson, G. A., Ayala, P. Y., Cui, Q., Morokuma, K., Malick, D. K., Rabuck, A. D., Raghavachari, K., Foresman, J. B., Cioslowski, J., Ortiz, J. V., Stefanov, B. B., Liu, G., Liashenko, A., Piskorz, P., Komaromi, I., Gomperts, R., Martin, R. L., Fox, D. J., Keith, T., Al-Laham, M. A., Peng, C. Y., Nanayakkara, A., Gonzalez, C., Challacombe, M., Gill, P. M. W., Johnson, B. G., Chen, W., Wong, M. W., Andres, J. L., Head-Gordon, M., Replogle, E. S., Pople, J. A. (1998) *Gaussian 98*, Gaussian, Inc., Pittsburgh, PA,
22. Nemeria, N., Baykal, A., Joseph, E., Zhang, S., Yan, Y., Furey, W., and Jordan, F. (2004) Tetrahedral intermediates in thiamin diphosphate-dependent decarboxylations exist as a 1′,4′-imino tautomeric form of the coenzyme, unlike the michaelis complex or the free coenzyme, *Biochemistry 43*, 6565−6575.
23. Littlechild, J., Turner, N., Hobbs, G., Lilly, M., Rawas, A., and Watson, H. (1995) Crystallization and preliminary X-ray crystallographic data with Escherichia coli transketolase, *Acta Crystallogr., Sect. D 51*, 1074−1076.
24. Otwinowski, Z., and Minor, W. (1997) Processing of X-ray diffraction data collected in oscillation mode, *Methods Enzymol. 276A*, 307−326.
25. Leslie, A. G. W. (1992) Recent changes to the MOSFLM package for processing film and image plate data, *Joint CCP4 + ESF-EAMCB Newsletter on Protein Crystallography*, No. 26.
26. Collaborative Computational Project Number 4 (1994) The CCP4 suite: programs for protein crystallography, *Acta Crystallogr., Sect. D 50*, 760−763.

27. Emsley, P., and Cowtan, K. (2004) Coot: model-building tools for molecular graphics, *Acta Crystallogr., Sect. D 60*, 2126−2132.
28. DeLano, W. L. (2002) The PyMOL Molecular Graphics System, DeLano Scientific, San Carlos, CA. http://www.pymol.org.
29. Fiedler, E., Golbik, R., Schneider, G., Tittmann, K., Neef, H., König, S., and Hübner, G. (2001) Examination of donor substrate conversion in yeast transketolase, *J. Biol. Chem. 276*, 16051−16058.
30. Gorbach, Z. V., and Kubyshin, V. L. (1989) Kinetic properties of transketolase from the rat liver in a reaction with xylulose-5-phosphate and ribose-5-phosphate, *Biokhimiia (Moscow) 54*, 1980−1985.
31. Gyamerah, M., and Willets, A. J. (1997) Kinetics of overexpressed transketolase from *Escherichia coli* JM 107/pQR 700, *Enzyme Microb. Technol. 20*, 127−134.
32. Machius, M., Wynn, R. M., Chuang, J. L., Li, J., Kluger, R., Yu, D., Tomchick, D. R., Brautigam, C. A., and Chuang, D. T. (2006) A versatile conformational switch regulates reactivity in human branched-chain alpha-ketoacid dehydrogenase, *Structure 14*, 287−298.
33. Berthold, C. L., Toyota, C. G., Moussatche, P., Wood, M. D., Leeper, F., Richards, N. G., and Lindqvist, Y. (2007) Crystallographic snapshots of oxalyl-CoA decarboxylase give insights into catalysis by nonoxidative ThDP-dependent decarboxylases, *Structure 15*, 853−861.
34. Nakai, T., Nakagawa, N., Maoka, N., Masui, R., Kuramitsu, S., and Kamiya, N. (2004) Ligand-induced conformational changes and a reaction intermediate in branched-chain 2-oxo acid dehydrogenase (E1) from Thermus thermophilus HB8, as revealed by X-ray crystallography, *J. Mol. Biol. 337*, 1011−1033.
35. Lobell, M., and Crout, D. H. G. (1996) Pyruvate decarboxylase: a molecular modeling study of pyruvate decarboxylation and acyloin formation, *J. Am. Chem. Soc. 118*, 1867−1873.
36. Friedemann, R., and Breitkopf, C. (1996) Theoretical studies on the decarboxylation reaction in thiamin catalysis, *Int. J. Quant. Chem. 57*, 943−948.
37. Cavazza, C., Contreras-Martel, C., Pieulle, L., Chabriere, E., Hatchikian, E. C., and Fontecilla-Camps, J. C. (2006) Flexibility of thiamine diphosphate revealed by kinetic crystallographic studies of the reaction of pyruvate-ferredoxin oxidoreductase with pyruvate, *Structure 14*, 217−224.
38. Frank, R. A., Titman, C. M., Pratap, J. V., Luisi, B. F., and Perham, R. N. (2004) A molecular switch and proton wire synchronize the active sites in thiamine enzymes, *Science 306*, 872−876.
39. Seifert, F., Golbik, R., Brauer, J., Lilie, H., Schröder-Tittmann, K., Hinze, E., Korotchkina, L. G., Patel, M. S., and Tittmann, K. (2006) Direct kinetic evidence for half-of-the-sites reactivity in the E1 component of the human pyruvate dehydrogenase multienzyme complex through alternating sites cofactor activation, *Biochemistry 45*, 12775−12785.
40. Bürgi, H. B., Dunitz, J. D., and Shefter, E. (1973) Geometrical reaction coordinates. II. Nucleophilic addition to a carbonyl group, *J. Am. Chem. Soc. 95*, 5065−5067.
41. Benkovic, S. J., and Hammes-Schiffer, S. (2003) A perspective on enzyme catalysis, *Science 301*, 1196−1202.
42. Garcia-Viloca, M., Gao, J., Karplus, M., and Truhlar, D. G. (2004) How enzymes work: analysis by modern rate theory and computer simulations, *Science 303*, 186−195.
43. Hur, S., and Bruice, T. C. (2003) The near attack conformation approach to the study of the chorismate to prephenate reaction, *Proc. Natl. Acad. Sci. U.S.A. 100*, 12015−12020.
44. Lau, E. Y., Kahn, K., Bash, P. A., and Bruice, T. C. (2000) The importance of reactant positioning in enzyme catalysis: a hybrid quantum mechanics/molecular mechanics study of a haloalkane dehalogenase, *Proc. Natl. Acad. Sci. U.S.A. 97*, 9937−9942.
45. Jencks, W. P. (1975) Binding energy, specificity, and enzymic catalysis: The circe effect, *Adv. Enzymol. Relat. Areas Mol. Biol. 43*, 219−410.
46. Wu, N., Mo, Y., Gao, J., and Pai, E. F. (2000) Electrostatic stress in catalysis: structure and mechanism of the enzyme orotidine monophosphate decarboxylase, *Proc. Natl. Acad. Sci. U.S.A. 97*, 2017−2022.

BI700844M